

Soft Matter

Accepted Manuscript



This is an *Accepted Manuscript*, which has been through the Royal Society of Chemistry peer review process and has been accepted for publication.

Accepted Manuscripts are published online shortly after acceptance, before technical editing, formatting and proof reading. Using this free service, authors can make their results available to the community, in citable form, before we publish the edited article. We will replace this *Accepted Manuscript* with the edited and formatted *Advance Article* as soon as it is available.

You can find more information about *Accepted Manuscripts* in the [Information for Authors](#).

Please note that technical editing may introduce minor changes to the text and/or graphics, which may alter content. The journal's standard [Terms & Conditions](#) and the [Ethical guidelines](#) still apply. In no event shall the Royal Society of Chemistry be held responsible for any errors or omissions in this *Accepted Manuscript* or any consequences arising from the use of any information it contains.

Friction of polymer hydrogel studied by resonance shear measurements

Huai-Yin Ren,^a Masashi Mizukami,^b Tadao Tanabe,^b Hidemitsu Furukawa,^c Kazue Kurihara^{*a,b}

^aWPI-Advanced Institute for Materials Research, Tohoku University, 2-1-1 Katahira, Aoba-ku, Sendai 980-8577, Japan, ^bInstitute of Multidisciplinary Research for Advanced Material, Tohoku University, 2-1-1Katahira, Aoba-ku, Sendai 980-8577, Japan and ^cGraduate School of Science and Engineering, Yamagata University, 4-3-16 Jonan, Yonezawa 992-8510, Japan.

Correspondence and requests for materials should be addressed to K.K. (email: kurihara@tagen.tohoku.ac.jp; Tel: 022-217-6253; Fax: 022-217-6154.)

ABSTRACT

The friction between an elastomer and a hard surface typically has two contributions; i.e., the interfacial and deformation components. The friction of viscoelastic hydrogel materials has been extensively studied between planar gel and planar substrate surfaces from the viewpoint of an interfacial interaction. However, the geometry of the contact in practical applications is much more complex. The geometric and elastic deformation term of a gel to friction could not be neglected. In this study, we used the resonance shear measurements (RSM) for characterizing the shear response of a glass sphere on a flat polymer hydrogel, a

double network (DN) gel of 2-acrylamide-2-methylpropanesulfonic acid and *N,N*-dimethylacrylamide. The contact mechanics conformed to the Johnson-Kendall-Roberts theory. The observed resonance curves exhibited rather sharp peaks when the DN gel and silica sphere were brought into contact, and its intensity and frequency increased with the increasing normal load. We proposed a simple physical model of the shearing system, and the elastic (k_2) and viscous (b_2) parameters of the interface between a silica sphere and a flat DN gel were obtained. The friction force from elastic deformation and viscous dissipation terms were then estimated using the obtained parameters. It was revealed that the elastic parameter (k_2) increased up to 1780 N/m at the normal load of 524 mN, while the viscous parameter (b_2) was zero or quite low (< 0.1 Ns/m) for a silica sphere (radius of 18.4 μ m). Thus, the friction force between a flat DN gel and a silica sphere in air was dominated by the elastic term due to the local deformation by contact with a silica sphere. By adding water, the elastic parameter (k_2) remained the same and the viscous parameter (b_2) slightly increased. However, the viscous term f_{viscous} was still much smaller than f_{elastic} . To the best of our knowledge, this study was the first quantitative estimation of the elastic deformation term to the friction in the case when deformation of non-flat contact regions occurs. The obtained results can be basic knowledge for designing gels for applications such as artificial cartilages and sliding bearings.

I. Introduction

A polymer hydrogel consists of a viscoelastic cross-linked polymer network in which water fills the interstitial space. The gel is a wet and soft material, and capable of undergoing a large deformation under an applied external force. One of the fascinating properties of the hydrogel is its excellent lubrication. The friction coefficient of the hydrogel could be as low as 10^{-3} or less,¹⁻³ and was comparable to that of some biological surfaces such as human and animal cartilages. However, the most common hydrogels are too fragile for practical applications. Recently, the hydrogels^{4,5}, which exhibit excellent mechanical properties, have been developed, e.g., a double network (DN) gel⁴ and nanocomposite hydrogel⁵. Therefore, practical applications of hydrogels as lubricants have become promising. For such applications, the understanding and the optimization of the friction of the gels have been important issues.

The friction force between an elastomer such as a gel and a hard surface involves two contributions commonly described as the surface interactions and deformation, respectively.^{6,7} To date, the friction of polymer hydrogels have been mainly studied between two planar surfaces from the viewpoint of surface interactions.¹⁻⁴ To elucidate the low friction mechanism, Gong and coworkers⁸ have proposed the repulsion–adsorption model. The surface polymer network will be repelled from the substrate surface if the interfacial interaction is repulsive, and will be adsorbed on the substrate surface if it is attractive. The lack of consideration in the deformation term is probably because most of the studies treated a planar gel and a planar substrate, thus, the interaction term dominated in the friction. Another reason is perhaps the lack of a suitable measurement technique for characterizing the deformation term. Kurokawa⁹ investigated the effect of the topographical elastic properties of crosslinked poly(*N, N*-dimethylacrylamide) hydrogels on their frictional properties by AFM. They demonstrated that the surface roughness and surface elastic

modulus have little influence on the surface friction. However, the deformation was limited to a nano- or micro-scale by the measurement technique. Mori and coworkers¹⁰ studied the friction properties of a poly(acrylic acid) hydrogel using a ball-on-plate tester in air and in water. They noticed that the penetration depth of the slider into the gel changed during the loading possibly modified the friction. However, the relation between deformation of gel and friction was not systematically clarified.

Kurihara and coworkers¹¹⁻¹³ have developed resonance shear measurements (RSM) using the surface force apparatus (SFA) and investigated the rheological and tribological properties of confined liquids in nanoscale spaces. The resonance response confers the measurement with a high sensitivity and stability. The frequency and the amplitude of the resonance shear response change depending on the surface separation, the thickness of confined liquids. By analyzing the resonance shear curves on basis of a proposed physical model, the properties such as viscosity,^{14,15} structuring,^{16,17} lubricity and friction¹⁸⁻²⁰ of the confined liquid are quantitatively evaluated. The RSM could also be used to investigate the viscoelastic and frictional properties of soft and solid materials.

In this study, we use the RSM apparatus combined with an optical microscope to study the frictional properties of the PAMPS (poly(2-acrylamide-2-methylpropanesulfonic acid))/PDMAAm (poly(*N, N*-dimethylacrylamide)) DN gel against a silica sphere (Fig.1). Here, PAMPS stands for poly(2-acrylamide-2-methylpropanesulfonic acid) and PDMAAm for poly(*N, N*-dimethylacrylamide). The deformation of the contacting area was monitored using the optical microscope. The contact mechanics conformed to the JKR theory. The observed resonance curves exhibited interesting peak shift and intensities changes in response to the contact, the applying load and the introduction of water. Finally, we clarified the geometrical and dynamic deformation terms to the gel friction by proposing a physical model and theoretically determining the friction force based on the model.

II. Experimental

Chemicals. The reagents were all provided by Wako Pure Chemical Industries, Ltd., Japan. The monomer, 2-acrylamido-2-methylpropanesulfonic acid (AMPS), was used as received. The monomer, *N,N*-dimethylacrylamide (DMAAm), was purified by filtering through an activated alumina column. *N,N'*-methylenebis(acrylamide) (BIS) and 2-oxoglutaric acid (α -keto) were used without further purification as the crosslinking agent and photo-initiator, respectively. Ultrapure water (Barnstead, NANOpure DIamond) was used after double distillation.

Synthesis of DN gel. The gel was synthesized according to a previous report.⁴ In short, the PAMPS gel was first synthesized by the photoinitiated free radical polymerization of 1 M monomer AMPS aqueous solutions containing 4 mol% BIS and 0.1 mol% α -keto against the monomer, between a pair of glass plates with a 2-mm spacing. The formed PAMPS gel was then immersed in an aqueous solution of 2 M DMAAm containing 0.1 mol% BIS and 0.1 mol% α -keto for two days until the swelling equilibrium was reached. Finally, the DN gel was formed by UV irradiation for another 24 hours. The as-prepared DN gel was then immersed in a large amount of pure water until the swelling equilibrium was reached. The width, length and thickness of the DN gel used for the measurement were about 10 mm, 10 mm and 3 mm, respectively.

Apparatus for contact mechanics and resonance shear measurements (RSM). The experimental apparatus is schematically illustrated in Fig.1. The RSM apparatus has been used to study the rheological and tribological properties of confined liquids in a nanospace.¹¹⁻

²⁰ In this study, the apparatus was used for both contact mechanics studies and resonance shear measurements between a silica sphere and a planar DN gel. The silica sphere (upper surface) was connected to the four-sectored piezotube and hung by a pair of vertical leaf springs ($k = 786$ N/m). A silica sphere ($R = 18.4$ mm or 6.9 mm) (Sigma-koki, Ltd., Japan)

was used. The silica spheres were cleaned using a “piranha” solution (a mixture of concentrated H_2SO_4 and 30% H_2O_2 (7/3 (v/v)) at 100 °C for 30 min, then thoroughly rinsed with pure water and with ethanol, then dried in an N_2 (g, purity > 99.99995 vol.%) stream prior to use. (*Caution: The piranha solution reacts violently with organic compounds*). The planar DN gel (lower surface) was mounted on a square holder, which was connected to the lower horizontal double-cantilever spring (the vertical spring constant, $K_v = 1084$ N/m or 250 N/m).

Contact mechanics measurements. A schematic drawing of the contact is found in the dotted frame in Fig. 1. The two surfaces were brought into contact by the pulse-motor driven movement of the lower surface (gel) in the vertical direction. Due to the difference in their stiffness, the rigid silica sphere was pressed onto the soft gel forming a contacting interface. A white light was directed into the chamber from the bottom. A CCD camera combined with the optical microscope (Olympus, BXFM) was placed on the top of the chamber to capture the contact image. Upon the initial contact, the contacting area spread quickly and finally reached a mechanical equilibrium state. The normal load can be applied by further movement of the springs. The pressing depth, h , was determined as

$$h = R - \sqrt{R^2 - r^2} \quad (1)$$

where R and r are the radius of the silica sphere and the contacting spot, respectively. The normal load, L , was determined as

$$L = \left[K_v (D_c - D) - (h - h_c) \right] \quad (2)$$

where D and D_c are the vertical displacement of the pulse-motor at normal load L and initial contact, respectively; h and h_c are the pressing depth at the normal load L and initial contact, respectively. The applied normal load at the initial contact was defined as 0 mN.

Changes in the contacting area (S) vs. the applied load (L) for a complete loading/unloading cycle were measured. The loading and unloading were carried out in a stepwise manner. The contacting areas at all the normal loads were measured after no visible changes in the areas were established, except the one just before the jump-out. The contacting area just before the jump-out was obtained from the video analysis. The contact mechanics was analyzed in terms of the Johnson–Kendall–Roberts (JKR) theory²¹. The JKR equation for this geometry is

$$S = \pi r^2 = \pi \left\{ \frac{3R}{4E} \left[L + 3\pi RW \pm \sqrt{6\pi RWL + (3\pi RW)^2} \right] \right\}^{2/3} \quad (3)$$

where E was the elastic modulus of the gel; W was the surface energy per unit area.

RSM for gels. The RSM was carried out using the same apparatus as shown in Fig.1. The upper unit was laterally oscillated by inputting sinusoidal voltages (amplitude $U_{in} = \pm 1$ V, frequency f typically within the range of 10–100 Hz) to the two opposite electrodes of the four-sectored piezotube using the DAQ (data acquisition) board from National Instruments. The movement of the vertical leaf springs (Δx) was detected using a capacitance probe (Microsense3401HR, Japan ADE, Ltd.) as its output voltage (U_{out} , sensitivity: 2.518 $\mu\text{m}/\text{V}$). The plot of the normalized amplitude (U_{out}/U_{in}) as a function of the angular frequency (ω) represents the resonance curve, which reflects viscoelastic properties of the interfacial contacting area. For most of the measurements, a double cantilever-spring with $K_v = 1084$ N/m was used. To check effect of the spring stiffness, one more pair of springs ($K_v = 250$ N/m) was used for comparison. The silica sphere and gel surfaces were exposed to the air or a droplet of pure water (about 1 μL), which was injected between the surfaces using a syringe to study the effect of water. All measurements were conducted at room temperature (21.0 ± 0.5 °C).

Analysis of resonance curves. The resonance curves were analyzed based on a physical model shown in Fig. 2. A similar model was previously reported for analyzing the resonance curve data obtained for liquids confined between two solid surfaces (see supplementary Fig. S1).²² The motions of the upper and lower surfaces were described by the equations of motion (eqn (4) and (5)).

$$m_1 \frac{d^2 x_1}{dt^2} + k_1 \frac{x_1}{\alpha} + k_2 (x_1 - x_2) + b_1 \frac{dx_1}{dt} + b_2 \frac{d}{dt} (x_1 - x_2) = F \exp(i\omega t) \quad (4)$$

and

$$m_2 \frac{d^2 x_2}{dt^2} + k_2 (x_2 - x_1) + k_3 x_2 + b_2 \frac{d}{dt} (x_2 - x_1) + b_3 \frac{dx_2}{dt} = 0 \quad (5)$$

where m_1 , k_1 and b_1 are the effective mass, elastic parameter and viscous parameter of the upper unit. The parameters k_2 and b_2 are the elastic and viscous parameters of the interface of the gel and spherical silica, respectively. The parameters of m_2 , k_3 and b_3 were the effective mass, elastic parameter and viscous parameter of the bulk gel mounted on the lower unit, respectively.

An analytical solution of the resonance curve (eqn (6)) was obtained by solving the equations of motion for the upper and lower surfaces (eqn (4) and (5)), and was used to determine the parameters of the DN gel-silica interface.

$$\frac{U_{\text{out}}}{U_{\text{in}}} = \frac{C}{\alpha} \sqrt{\frac{(K_2 - m_2 \omega^2)^2 + \omega^2 B_2^2}{[(K_1 - m_1 \omega^2)(K_2 - m_2 \omega^2) - \omega^2 B_1 B_2 - k_2^2 + b_2^2 \omega^2]^2 + \omega^2 [(K_1 - m_1 \omega^2) B_2 + (K_2 - m_2 \omega^2) B_1 - 2k_2 b_2]^2}} \quad (6)$$

where $B_1 = b_1/\alpha + b_2$, $B_2 = b_2 + b_3$, $K_1 = k_1/\alpha + k_2$, $K_2 = k_2 + k_3$. C is an intensity parameter.

The parameter α was defined as $\alpha = x_1/x_{\text{measured}}$. The typical α value ($\alpha = 1$) measured for the air separation (AS) was used for analyzing the resonance peaks measured before the gel-silica contact. The typical α value ($\alpha = 0.93$) measured for the mica contact was used for the peaks after the gel-silica contact. Originally, the parameters of m_2 , k_3 and b_3 represented the effective mass, elastic parameter and viscous parameter of the lower unit, respectively, which

consisted of the lower surface and lower spring.²¹ Because the gel exhibited an elastic deformation in response to the external force, we treated the bulk gel as an effective spring. Thus, in this study, the m_2 , k_3 , and b_3 parameters represented the mass, and the elastic and viscous parameters of the bulk DN gel, respectively. The parameters of the lower horizontal spring were not included in the physical model because the lower spring in the lateral direction (18000 N/m) was much stiffer than the bulk DN gel ($k_3 = 3830$ N/m)²³, resulting in the negligible deformation of the lower spring. It was confirmed that no change in the resonance peak was observed when the lower springs with different vertical spring constants were used (see supplementary Fig. S2).

Calculation of the friction. For convenience, the friction was estimated as the maximum driven force, which was transmitted from the forced sinusoidal oscillation of the upper surface to the lower surface. The amplitudes (X_1 and X_2) and the phase shifts (ϕ_1 and ϕ_2) of the upper and lower surfaces could be calculated using the determined parameters according to eqns (7) and (8).

$$\max |x_1 - x_2|_{peak} = \max |X_1 \exp(i\omega t + \phi_1) - X_2 \exp(i\omega t + \phi_2)|_{peak} \quad (7)$$

and

$$\max |V_1 - V_2|_{peak} = \max \left| \frac{dx_1}{dt} - \frac{dx_2}{dt} \right|_{peak} = \max |\omega X_1 \exp(i\omega t + \phi_1) - \omega X_2 \exp(i\omega t + \phi_2)|_{peak} \quad (8)$$

The maximum friction force f during a cycle of oscillation at a resonance peak frequency was estimated using the parameters k_2 and b_2 and the relative motions of the upper silica surface (x_1 , V_1) and lower DN gel (x_2 , V_2) according to eqn (9).

$$f = \max |f_{elastic} + f_{viscous}| = \max |-k_2(x_1 - x_2) - b_2(V_1 - V_2)| \quad (9)$$

We employed the maximum of the friction force as a representative value since the friction force continuously changed during an oscillation cycle.²⁶ The first and second terms of eqn

(9) were the displacement term due to the local deformation of the DN gel (f_{elastic}) and the velocity term due to the local viscosity of the interface between the DN gel and silica sphere (f_{viscous}), respectively.

III. Results and discussion

Contact mechanics between gel and silica. Before studying the friction mechanism by the RSM, we studied the contact mechanics between the flat DN gel and the spherical silica surface ($R = 18.4$ mm) using the set-up shown in Fig. 1. Fig. 3 shows a plot of the projected contacting area (S) vs. the applied load (L) measured for a complete loading-unloading cycle. The normal load L at the initial contact was defined as $L = 0$ mN. The loading and unloading were carried out in a stepwise manner. The contacting areas at all normal loads were measured after no visible changes in the areas were established, except the one just before the jump-out. The contacting area just before the jump-out was obtained from the video analysis. The contacting area increased with the increasing load. The S - L curves in the loading process and the unloading process were different, showing a clear hysteresis. The solid lines were the fitted results according to the Johnson-Kendall-Roberts (JKR) theory²¹ using eqn (3). The surface energy (W) and the elastic modulus (E) in the loading and unloading process were 0.086 ± 0.012 J/m² and 0.431 ± 0.004 J/m², and 665 ± 20 kPa and 884 ± 21 kPa, respectively. The hysteresis observed between the loading and unloading processes indicated the existence of a long-relaxation time scale during the deformation of the gel. This hysteresis may be related to both the surface interaction term²⁷ and the bulk deformation term²⁸. The increase in the compressed depth with the increasing load is shown in the inset of Fig. 3. The maximum depth pressed in this experiment, $h_{\text{max}} = 0.14$ mm at $L_{\text{max}} = 524$ mN, was only about 4.5% of the 3-mm thickness of the bulk gel. This ratio was low, however, the pressing depth and the deformation shape may affect the values for the

effective elastic modulus. Thus, we measured the S - L curves for the loading process using the same gel with a 3-mm thickness and a smaller silica sphere with $R = 6.9$ mm (see supplementary Fig. S3). The maximum depth deformed, $h_{\max} = 0.42$ mm at $L_{\max} = 1157$ mN, was about 14% of the 3-mm gel thickness. It was found that the E ($= 650$ kPa) for the loading process was practically constant within the experiment error (Fig. S3). These facts indicated that the effective modulus was constant and independent of the sphere radius and gel thickness in the loading range used in this experiment.

RSM for gels at various normal loads. To investigate the friction behavior by the RSM, the upper silica sphere ($R = 18.4$ mm) was laterally oscillated in the air in the closed chamber by applying a sinusoidal signal (U_{in}) into the piezotube (Fig.1). Fig. 4 shows the changes in the resonance curves of the upper mechanical unit when the upper silica sphere was in contact with the lower gel surface and further compressed by the applied normal load. The reference state, the curve for two surfaces separated in air (air separation, AS) was plotted for convenience. For the AS curve, the peak appeared at the frequency of 220 rad/s, which was determined by the mass and the spring constant of the upper unit. Upon the initial contact of the silica sphere and gel ($GC_{(0)}$), the resonance curves of the upper mechanical unit showed a significant shift in the frequency from AS (220 rad/s) to $GC_{(0)}$ (255 rad/s). The normal load L at this initial contact $GC_{(0)}$ was defined as 0 mN. The amplitudes of the AS peak and $GC_{(0)}$ peak were 9.8 and 6.6, respectively. With a further increase in the normal load, the peak continuously shifted and the intensities monotonically increased. For example, at the maximum applied load ($L = 524$ mN), the frequency shift increased from 255 rad/s to 308 rad/s and the intensity increased by 218% to 21 from 6.6 of the $GC_{(0)}$ peak. The shift in frequency and the increase in amplitude may arise from the increase in the elastic deformation of gel against the silica sphere when compressed by the loads. The mechanism will be discussed in detail later.

Next, we studied the effect of the sphere radius on the resonance curves using a silica sphere of $R = 6.9$ mm. The resulting changes in the resonance curves as a function of the normal load are shown in Fig. 5a. The curves exhibited a similar trend (initial jump and the subsequent and continuous increase in both the frequency and the amplitude) when the silica sphere was in contact with the lower gel and compressed by the applied load. However, both the frequencies and amplitudes exhibited higher values than those using the silica sphere of $R = 18.4$ mm. This result could be attributed to the higher applied pressures for smaller spheres for identical normal loads (Fig. 5b).

Effect of the addition of water. Water has been used as a lubricant in cases of gel lubrication.^{12,29} To check the effect of water, a droplet (1 μ L) of water was added between the two surfaces. Fig. 6 shows the changes in the resonance curves as a function of the normal load in the case of using a silica sphere of $R = 18.4$ mm. The data for using a silica sphere of $R = 6.9$ mm is shown in Fig. S4. It should be noted that the contacting area could not be well distinguished by the optical microscope due to the presence of a water film. Therefore, the normal load could not be experimentally measured. To estimate the normal load (L), we assumed that the angular frequencies of the resonance peaks (ω) were mainly determined by the elastic deformation of the gel (k_2), which was directly related to the contacting areas (S) at various normal loads (L). We plotted the angular frequency (ω) vs. the contacting area (S) curve from the RSM data obtained without the addition of water and applied a mathematical fitting (see supplementary Fig. S5a). By using the obtained ω - S function, we then estimated the values of the contacting areas (S) for each resonance curve measured with the addition of water. Since the contact mechanics was well described by the JKR theory, we then determined the normal load (L) for various contacting areas using eqn (3) (see supplementary Fig. S5b).

In the presence of a significant thickness of water between the silica sphere and gel surfaces, the RSM curve initially appeared at the same frequency as the AS peak (Fig. 6a-(i)). By moving the gel surface to the silica surface, the resonance curves exhibited a drastic decrease in the amplitude and a gradual shift in the frequency from curves-(i) to (ii), (ii) and (iii) (Fig. 6a). At curve (iv), the peak almost disappeared and the frequency shifted to 252 rad/s. With a further applied normal load, the curves started to rise, and continuously shifted to the high frequency range. For example, the frequency and amplitude of the peak increased to 310 rad/s and 13, respectively, at $L = 438$ mN. The large elastic deformation caused by the high normal load should be responsible for the changes. However, it should be emphasized that the peaks in intensity showed a clear reduction compared to those without the addition of water (Fig. 6b). A thin water layer could have remained between the interfaces, which reduced the friction between the surfaces.

Analysis of the resonance shear curves. To understand the physical meaning of the changes in the resonance shear curves, the experimental curves were analyzed by eqn (6). The theoretical fit curves at various normal loads L are shown in Fig. S6 as examples together with the fitting parameters b_2 and k_2 for the measurements on the silica sphere of $R = 18.4$ mm without the addition of water. The parameters b_1 , b_3 , k_1 and k_3 were fixed at 0.08 Ns/m, 0 Ns/m, 1102 N/m and 3830 N/m, respectively. The b_2 and k_2 values are summarized in Table 1 together with those obtained for other measurements. Without the addition of water, the viscous parameter b_2 was zero in the whole normal load L range ($L \leq 525$ mN) for the silica sphere of $R = 18.4$ mm, and at $L \leq 749$ mN for the sphere of $R = 6.9$ mm. The b_2 values for the cases with added water were in the range of 0.01 ~ 0.12 within the applied load range. The increase in the viscous damping parameter b_2 by the addition of water indicated that the water layer remained between the silica sphere and the DN gel, and the oscillation energy dissipated within the layer. In the case of the 6.9 mm sphere at a high normal load, even

without the addition of water, the b_2 value increased to 0.03 Ns/m at 1157 mN and 0.05 Ns/m at 1597 mN. This result should indicate that water was squeezed from the inside of the gel to the interface region due to the higher normal pressure.

To examine the effect of the normal load as well as the addition of water on the elastic parameter k_2 , the k_2 values were plotted versus L for both with and without the addition of water. The double logarithmic plots of k_2 vs. L in Fig. 7 showed linear relations for all the cases indicating that the $k_2(L)$ follows a power law function ($k_2(L) = a L^n$, a : intensity parameter). The plots for the spheres of the same radius R were practically identical with and without the addition of water, indicating that the elastic deformation of the gel at the same normal load was not changed by the addition of water.³⁰ The power index n for the $R = 6.9$ mm sphere, 0.49 (without water) and 0.50 (with water) was larger than that for $R = 18.4$ mm, $n = 0.31$ (without water) and 0.29 (with water). This result could be explained by the different deformation degree of the DN gel using silica spheres of different radii; the deformation depth (h) of the DN gel in contact with the smaller sphere ($R = 6.9$ mm) was greater than that in contact with the larger sphere ($R = 18.4$ mm) for the same normal load.

Determination of the friction. The friction force mechanism between a silica sphere and a flat DN gel based on the friction force (f) was estimated using eqn (9) which contains the elastic deformation ($f_{\text{elastic}} = k_2|x_1-x_2|$) and viscous damping ($f_{\text{viscous}} = b_2|V_1-V_2|$) terms. The value $|x_1-x_2|$ was calculated using eq. (7) and shown in Fig. S7 as a function of L , and the value $|V_1-V_2|$ was using eq. (8). Fig. 8 showed the double-logarithmic plot of the calculated friction force and normal load (f vs. L) between the silica sphere–DN gel interface. For all the f vs. L plots, a linear relation was observed, indicating that $f(L)$ follows a power law function ($f(L) = a L^n$). The best fit $f(L)$ functions and the fitting lines are also shown in Fig.8.

In the case of the $R = 18.4$ mm silica sphere without the addition of water, the friction force f solely arose from the elastic deformation term $f = f_{\text{elastic}}$ because the viscous term f_{viscous} was zero (parameter $b_2 = 0$). When the water was added to the interface, the friction force became weaker in the entire normal load range because the $|x_1 - x_2|$ value was much smaller than those for without water as shown in Fig. S7. The energy dissipation through the lubrication by the water layer resulted in the decrease in the shear amplitude between the silica sphere and bulk DN gel, $|x_1 - x_2|$ (see Fig. S7), and thus the elastic deformation term $f_{\text{elastic}} = k_2|x_1 - x_2|$ decreased (Fig. 8).

A previously proposed mechanism of the decrease in the friction of the gel under water was the electrostatic repulsion between sliding surfaces, which maintained the hydrodynamic lubrication by water layer.³ In our results, the existence of the water layer between surfaces was also indicated in appearance of the b_2 value when the water was added to the interface (see Table 1). The maximum electrostatic repulsion we expect is about 10 mN/m (corresponds to 0.18 mN), which is much smaller than the difference in the applied normal load between the cases with and without water. Therefore, negative contribution of the repulsion to the applied pressure is only a part of causes of the reduction of the friction.

In the case of the $R = 6.9$ mm silica sphere, the friction force was greater than that obtained for the silica sphere of $R = 18.4$ mm over the entire normal load range. This higher friction was well correlated with the higher k_2 value due to the deeper and steeper deformation of the DN gel (Fig. 7). The reduction in the friction by the addition of water was also observed.

Friction behaviors of hydrogels significantly depended on the deformation degree of the gels in the case when a high large elastic deformation in the non-flat contact region occurs. Such a deformation term cannot be neglected for practical applications of hydrogels as

lubrication materials. The RSM is a very useful technique to characterize the viscoelastic properties of soft and solid materials and their correlation with the friction behaviors.

IV. Conclusion

The frictional properties of a polymer hydrogel (DN gel) sliding against a silica sphere were investigated by contact mechanics and resonance shear measurement (RSM). The contact mechanics conformed to the Johnson–Kendall–Roberts theory. The observed resonance curves exhibited the rather sharp peaks when the DN gel and silica sphere were brought into contact, and its intensity and frequency increased with the increasing normal load. We proposed a simple physical model of the shearing system, and the elastic (k_2) and viscous (b_2) parameters of the interface between a silica sphere and a flat DN gel were obtained. The friction force ($f = \max(|f_{\text{elastic}} + f_{\text{viscous}}|)$) from the elastic deformation (f_{elastic}) and viscous dissipation (f_{viscous}) terms were estimated using the obtained parameters. The results revealed the following.

(1) The friction force between a flat DN gel and a silica sphere (radius of 18.4 mm) in air was dominated by the elastic term (f_{elastic}) due to the local deformation by contact with a silica sphere. For a silica sphere with the smaller radius (6.9 mm), the friction force became higher due to the more significant deformation of the gel resulting in the higher elastic parameter k_2 .

(2) The elastic term (f_{elastic}) was dominant even when water was added to the interfaces because the elastic parameter (k_2) remained the same and the viscous parameter (b_2) only slightly increased. The elastic term decreased due to the smaller shear amplitude ($|x_1 - x_2|$) in the presence of water.

To the best of our knowledge, this study was the first quantitative estimation of the elastic deformation term to the friction force when a significant deformation of non-flat contact regions occurs. Such a deformation term cannot be neglected in practical applications of hydrogels as lubrication materials. The obtained results can be the basis for designing a gel for such applications. These results could also be the basis for the designing

of rubber-like elastic materials such as rubber tires. The RSM is a very useful technique to characterize the viscoelastic properties of soft and solid materials and their correlation with the friction behaviors.

Acknowledgements

This work was supported by the “Green Tribology Innovation Network” in the area of Advanced Environmental Materials of Green Network of Excellence (GRENE) program from the Ministry of Education, Culture, Sports, Science, and Technology of Japan.

V. References

- 1 J. Gong, M. Higa, Y. Iwasaki, Y. Katsuyama and Y. Osada, Friction of gels, *J. Phys. Chem. B*, 1997, **101**, 5487–5489.
- 2 J. Gong, Y. Iwasaki, Y. Osada, K. Kurihara and Y. Hamai, Friction of gels. 3. Friction on solid surfaces, *J. Phys. Chem. B*, 1999, **103**, 6001–6006.
- 3 J. P. Gong, Friction and lubrication of hydrogels-its richness and complexity, *Soft Matter*, 2006, **2**, 544–552.
- 4 J. P. Gong, Y. Katsuyama, T. Kurokawa and Y. Osada, Double-network hydrogels with extremely high mechanical strength, *Adv. Mater.*, 2003, **15**, 1155–1158.
- 5 K. Haraguchi and T. Takehisa, Nanocomposite hydrogel: a unique organic–inorganic network structure with extraordinary mechanical, optical, and swelling/de-swelling properties, *Adv. Mater.*, 2002, **14**, 1120–1124.
- 6 B. J. Briscoe and S. K. Sinha, Wear of polymers, *Proc. Inst. Mech. Eng. J J. Eng. Tribol.*, 2002, **216**, 401–413.
- 7 N. K. Myshkin, M. I. Petrokovets and A. V. Kovalev, Tribology of polymers: Adhesion, friction, wear, and mass-transfer, *Tribol. Int.*, 2005, **38**, 910–921.
- 8 J. Gong, and Y. Osada, Gel friction: A model based on surface repulsion and adsorption, *J. Chem. Phys.*, 1998, **109**, 8062–8068.
- 9 T. Kurokawa, J. P. Gong and Y. Osada, Substrate effect on topographical, elastic, and frictional properties of hydrogel, *Macromolecules*, 2002, **35**, 8161–8166.
- 10 X. Liu, H. Nanao, T. Li and S. Mori, A study on the friction properties of PAAc hydrogel under low loads in air and water, *Wear*, 2004, **257**, 665–670.
- 11 C. D. Dushkin, and K. Kurihara, Nanotribology of thin liquid-crystal films studied by the shear force resonance method, *Colloids Surf. A: Physicochem. Eng.*, 1997, **129–130**, 131–139.

- 12 C. D. Dushkin, K. Kurihara, A resonance shear force rheometer modeled as simple oscillating circuit, *Rev. Sci. Instrum.*, 1998, **69**, 2095–2104.
- 13 H. Sakuma and K. Kurihara, Fourier-transform resonance shear measurement for studying confined liquids, *Rev. Sci. Instrum.*, 2009, **80**, 013701.
- 14 Y. Kayano, H. Sakuma and K. Kurihara, Nanorheology of dioctyl phthalate confined between surfaces coated with long alkyl chains, *Langmuir*, 2007, **23**, 8365–8370.
- 15 M. Mizukami, K. Kusakabe and K. Kurihara, Shear resonance measurement on structuring of liquids confined between mica surfaces, *Progr. Colloid Polym. Sci.*, 2004, **128**, 105–108.
- 16 K. Ueno, M. Kasuya, M. Watanabe, M. Mizukami and K. Kurihara, Resonance shear measurement of nanoconfined ionic liquids, *Phys. Chem. Chem. Phys.*, 2010, **12**, 4066–4071.
- 17 H. Sakuma, K. Otsuki and K. Kurihara, Viscosity and lubricity of aqueous NaCl solution confined between mica surfaces studied by shear resonance measurement, *Phys. Rev. Lett.*, 2006, **96**, 046104.
- 18 H. Mizuno, T. Haraszti, M. Mizukami and K. Kurihara, Nanorheology and nanotribology of two-component liquid crystal, *SAE Int. J. Fuels Lubr.*, 2009, **1**, 1517–1523.
- 19 M. Kasuya, M. Hino, H. Yamada, M. Mizukami, H. Mori, S. Kajita, T. Ohmori, A. Suzuki, and K. Kurihara, Characterization of water confined between silica surface using the resonance shear measurement, *J. Phys. Chem. C*, 2013, **117**, 13540–13546.
- 20 J. Watanabe, M. Mizukami, K. Kurihara, Resonance Shear Measurement of Confined Alkylphenyl Ether Lubricants, *Tribol. Lett.*, 2014, **56**, 501-508.

- 21 H. Yoshizawa, Y.-L. Chen and J. Israelachvili, Fundamental mechanisms of interfacial friction. 1. Relation between adhesion and friction, *J. Phys. Chem.*, 1993, **97**, 4128–4140 (1993).
- 22 M. Mizukami and K. Kurihara, A new physical model for resonance shear measurement of confined liquids between solid surfaces, *Rev. Sci. Instrum.*, 2008, **79**, 113705.
- 23 The typical lateral spring constant of the lower spring used in this study was ca. 18000 N/m and much higher than that for the shear deformation of the bulk DN gel (3830 N/m) estimated from Young's modulus and the size of the DN gel. The shear force (F) for the deformation (Δx) of a material with a thickness t , area A and a shear modulus G can be written as $F = GA\Delta x/t$. According to Hooke's law, the shear force (F) for the deformation of the DN gel with a lateral spring constant of k_3 is defined as $F = k_3\Delta x$. From these equations of shear forces, an equation for k_3 can be written as $k_3 = GA/t = EA/((2(1 + \nu)t)$. Here, E is Young's modulus, and ν is the Poisson's ratio of the gel. The k_3 value of 3830 N/m was obtained using the size of the DN gel ([width, length and thickness were 10 mm, 10 mm and 3 mm, respectively](#)), $E = 340$ kPa obtained from a tensile test measurement, and $\nu = 0.47$ which is a typical value for gels.^{24,25}
- 24 K. Urayama, T. Takigawa, T. Masuda, Poisson's Ratio of Poly(vinyl alcohol) Gels, *Macromolecules*, 1993, **26**, 3092-3096.
- 25 T. Takigawa, Y. Morino, K. Urayama, T. Masuda, Poisson's Ratio of Polyacrylamide (PAAm) Gels, *Polym. Gels. Netw.*, 1996, **4**, 1–5.
- 26 J. Peachey, J. V. Alsten, S. Granick, Design of an apparatus to measure the shear response of ultrathin liquid films. *Rev. Sci. Instrum.*, 1991, **62**, 463–472.
- 27 G. Y. Choi, S. Kim and A. Ulman, Adhesion hysteresis studies of extracted poly(dimethylsiloxane) using contact mechanics, *Langmuir*, 1997, **13**, 6333–6338.

- 28 G. Luengo, J. Pan, M. Heuberger and J. N. Israelachvili, Temperature and time effects on the “adhesion dynamics” of poly(butyl methacrylate) (PBMA) surfaces, *Langmuir*, 1998, **14**, 3873–3881.
- 29 K. Haraguchi and T. Takada, Characteristic sliding friction behavior on the surface of nanocomposite hydrogels consisting of organic-inorganic network structure, *Macromol. Chem. Phys.*, 2005, **206**, 1530–1540.
- 30 This result supported the assumption, not sufficient influence of b_2 on ω , for estimating the normal load L for the cases of added water using the frequency ω .

Table 1. Viscoelastic parameters determined for silica sphere/gel interfaces.

$R = 18.4 \text{ mm}$						$R = 6.9 \text{ mm}$					
No H ₂ O added			H ₂ O added			No H ₂ O added			H ₂ O added		
L	k_2	b_2	L	k_2	b_2	L	k_2	b_2	L	k_2	b_2
0	625	0	i	0	0.01	0	565	0	i	290	0.01
14.6	655	0	ii	0	0.12	62	1310	0	ii	445	0.01
36	800	0	iii	305	0.07	205	2200	0	5(iii)	607	0.01
77	978	0	iv	465	0.07	435	3210	0	42	1150	0.01
159	1250	0	14(v)	625	0.07	749	4300	0	120	1630	0.035
249	1430	0	55.6	875	0.055	1157	5380	0.03	188	2270	0.045
340	1575	0	129	1160	0.055	1597	6200	0.05	385	3230	0.11
429	1695	0	275	1505	0.04				617	4160	0.15
525	1775	0	438	1770	0.04				1000	5270	0.27

L : normal load (mN); k_2 : spring constant (N/m); b_2 : damping coefficient (Ns/m)

Figure Captions

Fig. 1 Schematic drawings of the resonance shear measurement system. The upper unit was laterally oscillated with a sinusoidal motion. The lower gel surface was brought into contact with the upper surface by vertical movement of the lower leaf springs. The response (deflection, Δx) of the upper unit was detected using a capacitance probe. The image within the dotted frame showed the normal deformation (pressing depth, h) of the gel surface caused by the rigidity difference. $h = R - \sqrt{R^2 - r^2}$, where R and r are the radius of the silica sphere and projected contacting area, respectively. The parameter r was obtained from the optical image of the contacting spot.

Fig. 2 (a) Physical model and (b) schematic drawings of the shearing system. The parameters b_1 and k_1 , b_2 and k_2 , b_3 and k_3 are the viscous coefficient and elastic parameters for the upper unit, silica sphere/gel interfaces and the bulk gel, respectively; m_1 and m_2 are the effective mass of the upper unit and polymer gels, respectively; x_1 and x_2 are the motion of the upper unit and lower polymer gels, respectively. The contribution of the lower horizontal springs was neglected because the lower springs did not contribute to the shape of the curves (see Fig. S2). Considering the shear deformation of the gel in the lateral direction, the bulk gel was treated as an effective spring, whose lateral spring constant k_3 was estimated to be 3830 N/m from the shape and Young modulus of the gel.²³

Fig. 3 Contact mechanics. Contacting area–normal load (S vs. L) curves for the silica sphere on the flat DN gel for a complete loading–unloading cycle. The gel surface was exposed to dry air in the closed RSM chamber. The contacting areas for all the normal loads were measured after no visible changes in the areas were established, except the one just before the

jump-out. The contacting area just before the jump-out was obtained from the video analysis. The symbols and the solid lines were the experimental data and fitting curves, respectively.

Fig. 4 RSM on gel using a silica sphere with $R = 18.4$ mm. Changes in the resonance shear curves as a function of the normal load for the silica sphere/gel interfaces without the addition of water between the two surfaces. Leaf springs with $K_v = 1084$ N/m were used as the lower horizontal double cantilever-spring.

Fig. 5 RSM on gel using a silica sphere with $R = 6.9$ mm. (a) Changes in the resonance shear curves as a function of the normal load for the silica sphere/gel interfaces without the addition of water between the two surfaces. (b) Comparisons of changes of frequency and amplitude as a function of normal load between cases using silica spheres with $R = 18.4$ mm and 6.9 mm. Leaf springs with $K_v = 1084$ N/m were used as the lower horizontal double cantilever-spring.

Fig. 6 Effect of the addition of water. (a) Changes in the resonance shear curves as a function of the normal load for the silica sphere/gel interfaces. (b) Summarized changes in amplitude and angular frequency with and without the addition of water. The silica sphere with $R = 18.4$ mm was used. Leaf springs with $K_v = 1084$ N/m were used as the lower horizontal double cantilever-spring. The estimation of S and L using the ω vs. S and S vs. L relations (Fig.S5a and Fig. S5b) did not apply to curves-(i), (ii), (iii) and (iv) because of the presence of water preventing the full contact of the gel and silica sphere unlike the case without the addition of water. The gel sample was moved upward by 10 μm , 10 μm , 10 μm , and 20 μm by the pulse motor from curve-(i) to (ii), (ii) to (iii), (iii) to (iv), and (iv) to (v), respectively.

Fig. 7 Calculated maximum friction forces acting across the silica sphere/gel interfaces at the resonance frequency as a function of the normal load.

Fig. 8 Plots of elastic parameter of gel and spherical silica interface (k_2) against normal load (L).

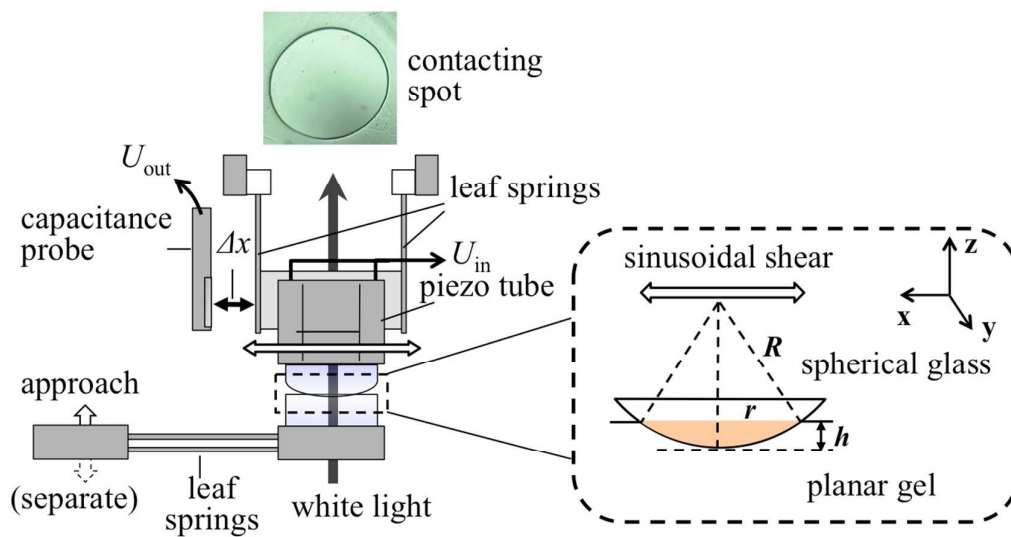
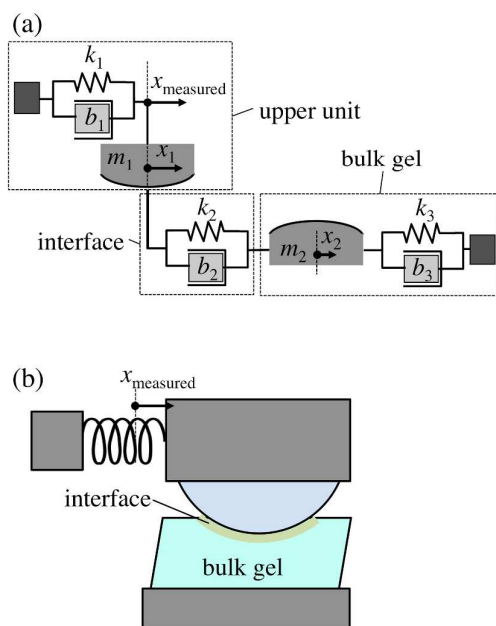
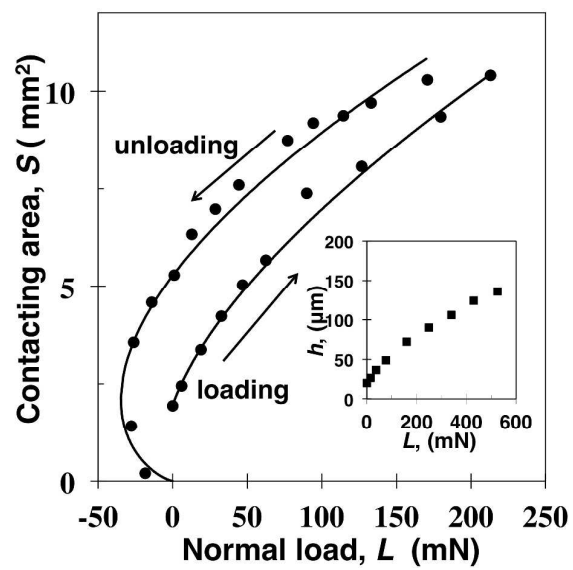
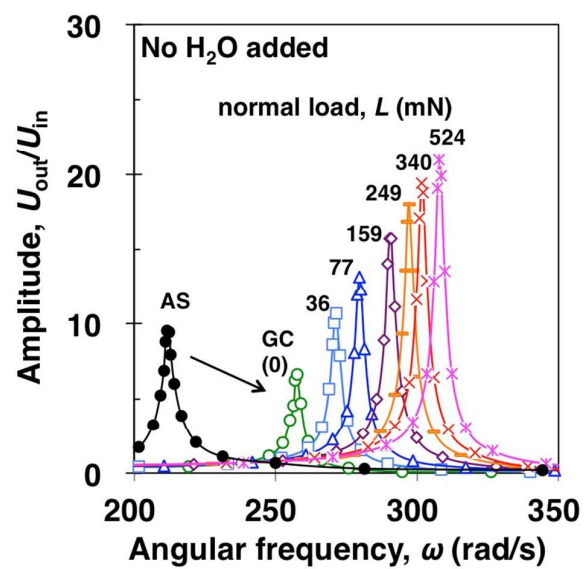


Fig. 1

**Fig. 2**

**Fig. 3**

**Fig. 4**

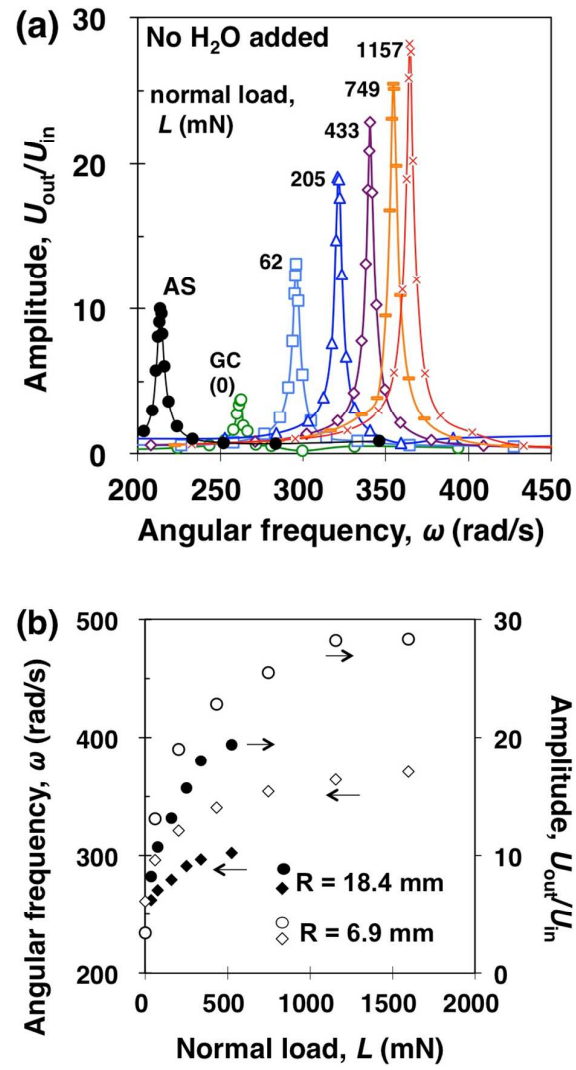


Fig. 5

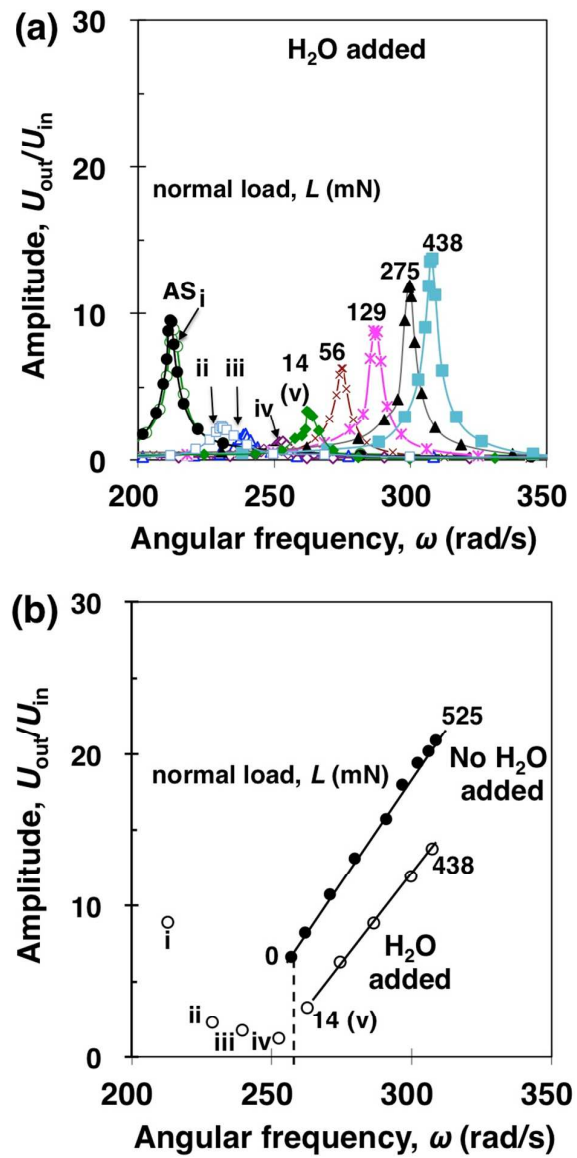
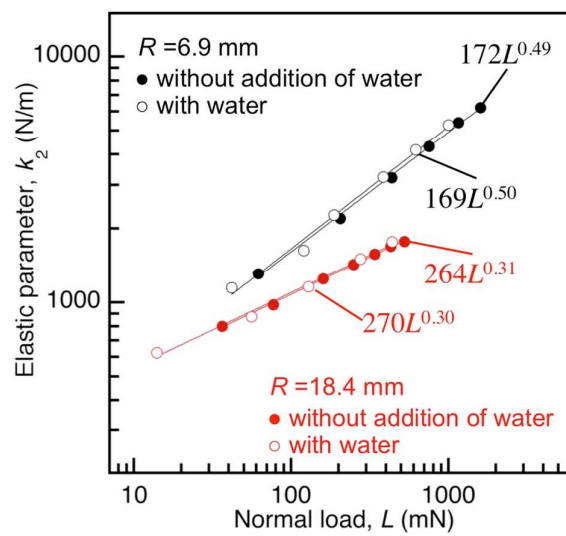
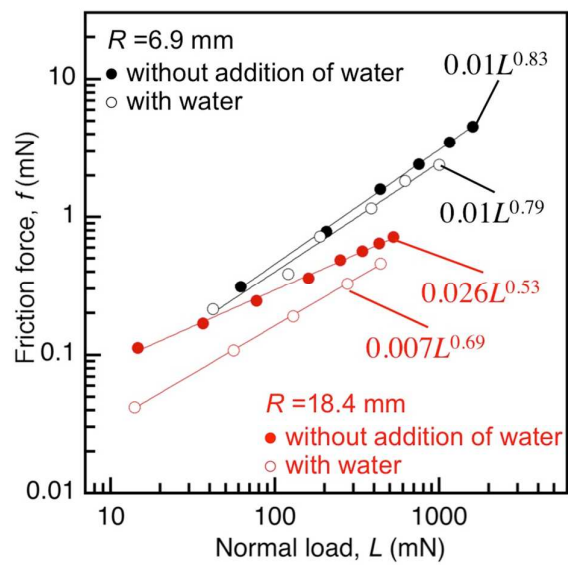


Fig. 6

**Fig. 7**

**Fig. 8**